TLOSHR Analysis of SMART-ITL using SPACE Code

Seung Wook Lee [a*], Jong Hyuk Lee [a], Sung Won Bae [a], Tae Wook Ha [a]
[a]*Korea Atomic Energy Research Institute, 989-111 Daedeok-daero, Yuseong-gu, Daejeon 3405, Rep. of Korea*
[*]*Corresponding author: nuclist@kaeri.re.kr*

1. Introduction

Based on the phenomena identification and ranking tables (PIRT) for SMART100 design extension conditions (DEC) [1], the thermal-hydraulic models of SPACE has been improved including special component such as a lumped cell model to simulate core makeup tank. In order to validate the capability of newly implemented components, total loss of secondary heat removal (TLOSHR) scenario among the representative accident scenarios of SMART-ITL [2] has been validated using improved SPACE in this study.

2. Methods and Results

2.1 TLOSHR Scenario

The TLOSHR of SMART-ITL starts by stopping all main feed water (FW) pumps. Normally passive residual heat removal system (PRHRS) will work and supply emergency feedwater to the SGs in such a case, however, it is assumed that no PRHRS will work in this scenario. Due to the complete loss of feedwater with PRHRS failure, the secondary system is isolated and the core makeup tanks (CMTs) are injected into reactor coolant system (RCS) except for loop #3 with single failure assumption. The RCS and the steam generator (SG) secondary begin to be pressurized due to power-cooling mismatch because the core heat removal via PRHRS is unavailable. When the RCS pressure reaches the high pressuirzer pressure (HPP), a reactor trip signal is generated, and the core heater power begins to decrease according to the decay heat table in the control logic. Afterwards, the RCS and the secondary system are depressurized due to relatively large heat loss of SMART-ITL compared with decay power. Consequently, pressurizer safety valve (PSV) to protect overpressure is not open.

The RCS is slowly cooled down by both of the CMT injection and the system heat loss and, reaches the saturation condition. Because there is no loss of coolant inventory, the volume of reactor coolant is only reduced by cooling effect and the water level of RCS is slowly decreased. In early phase of test, there is no CMT water level drop because forced circulation of single phase liquid flow is established through pressure balance line (PBL) and CMT injection lines as the level of the upper part of the reactor pressure vessel (RPV) downcomer is full and all reactor coolant pumps (RCPs) are operated. After the pressurizer (PZR) pressure reaches the setpoint of L-LPP, the safety injection tanks (SITs) except SIT #3 starts to operate. There is no blowdown of RCS coolant because both of the PSV and automatic depressurization system (ADS) are not open. The ADS is not open because the CMT level remains above the ADS open set point of 38%. The collapsed water level of the RCS is recovered again to almost initial level by CMT and SIT injection. Table I shows major sequence of event of the TLOSHR scenario for the SMART-ITL facility.

Table I: Sequence of Events in TLOSHR [3]

Event	Setpoint	Time (s)
Arrival of Steady State	-	0
TLOSHR start	FW stop PRHRAS generation all PRHRS failure	672
CMTAS	PRHRAS+1.45 s	674
CMT injection	CMTAS+1.45 s	675
MSIV / MFIV close	PRHRAS+5 s	677
Rx trip setpoint	PZR P=16.53 MPa	784
Rx trip signal (HPP)	HPP+1.1 s	785
Control rod insert	HPP+1.6 s	786
PSV open*	PZR P=17.27 MPa	-
PSV close	PZR P=13.87 MPa	-
ADS open*	38% level of CMT	-
RCP stop*	ADS open+10 min	-
SITAS	PZR P=L-LPP+1.45 s	97,562
SIT injection	SITAS+1.45 s	97,564

*PSV, ADS and RCP trip was not actuated during the test

2.2 Steady State Condition

The SMART-ITL facility is modeled as a single RPV and four SG components. These components are enveloped by the solid walls with heat losses through the surroundings. The surrounding ambient temperature is assumed as 303.15 K. The adiabatic passive safety injection system (PSIS) lines including CMTs and SITs are connected at upper downcomer of the RPV and MS lines are connected to the top of SG. The upper and lower annulus volumes in the RPV are modeled by using the single PIPE component with annulus option. While the SMART plant is an integral reactor and SGs are encapsulated in the RPV vessel, SMART-ITL is designed that the SGs are installed in exterior of the RPV and connected with pipe lines. The FW line connected to the SG inlet is also modeled and the feed water is supplied by TFBC component using flow boundary condition at constant flow rate.

The core heater power is set to 1,666 kW including heat loss. In addition, PZR heaters are also working in the steady state conditioning phase to maintain the target pressure. Each RCP speed is controlled to achieve the

appropriate core temperature difference. The PRHRS is excluded in the SPACE modeling because it is assumed that all PRHRSs are unavailable during the TLOSHR scenario.

Table II summarizes the steady calculation result of major parameters and deviations from the measured values.

Table II Steady Calculation Results of TLOSHR

	EXP [3]	SPACE	Err. (%)
Core Power (kW)	1,666	1,666	B.C.
Core inlet/outlet Temperature (K)	569.65	570.15	0.09
	594.75	595.14	0.07
SG primary inlet/outlet Temperature (K)	594.65	593.98	-0.11
	572.35	571.11	-0.22
RCS flowrate (kg/s)	10.177	11.48	Adjusted
PZR Pressure (MPa)	15.0	15.0	0.0
PZR water level (m)	3.064	3.061	-0.10
SG sec. inlet/outlet (K)	504.25	504.25	B.C.
	588.45	590.17	0.29
SG flow rate (kg/s)	0.761	0.768	Adjusted
FW Pressure (MPa)	5.71	5.71	B.C.
MS pressure (MPa)	5.62	5.64	0.36

2.3 Transient Results

Environmental heat loss is a key parameter determining the overall behavior of SMART-ITL during TLOSHR because a feed and bleed operation is unavailable and the only way to cool down the RCS is the heat loss through the structure of system in this scenario. Therefore, the heat loss coefficient of every heat structure should be properly adjusted to simulate the cool-down behavior of SMART-ITL. For this purpose, heat transfer coefficients for heat loss used for the transient calculation have been determined by sensitivity study.

Table III shows the summarized sequence of events of TLOSHR scenario predicted by the SPACE. SPACE predicts the earlier sequences such as the CMT actuation signal (CMTAS), MSIV / MFIV isolation, Rx trip and scram very well but shows delayed trends for later sequences such as the SIT injection. Similar to the experiment, there is no PSV / ADS actuation and no RCP stop in SPACE prediction. The SPACE calculation was terminated when the RCS condition reached the safe shutdown condition.

Table III: Predicted Sequence of Events of TLOSHR

Event	Time (EXP [3])	Time (SPACE)
TLOSHR start	672	672
PRHRAS generation	672	672
CMTAS	674	673.5
CMT injection	675	674.9
MSIV / MFIV close	677	677.0
Rx trip setpoint	784	777.8
Rx trip signal by HPP	785	778.9
Control rod insert	786	779.4
SITAS	97,562	100,099
SIT injection	97,564	100,100

Fig. 1 shows the comparison result of PZR pressure between experimental data and prediction by SPACE during entire calculation period. As soon as the feedwater supply to the SGs was terminated, PZR pressure was drastically increased due to loss of heat sink. As the RCS pressure reached the setpoint of HPP, a reactor trip signal was generated, and the core power started to decrease according to the programmed decay heat table in the control logic. After decrease of core power, the RCS and the secondary system began to be depressurized slowly due to a heat loss to environment and as a result, the PSV was not opened. The PZR pressure was continuously decreased as the RCS was cooled down by the CMT injection and heat loss and finally, reached the setpoint of SITAS. As shown in figure, the prediction result of SPACE agreed well with experiment data.

Fig. 2 shows the comparison of MSL pressure between experiment and SPACE prediction. As all MSIVs and MFIVs were closed with delay time of 5 seconds by the isolation signal PRHRAS, MSL pressure was suddenly increased up to peak pressure and then decreased due to heat loss to environment in short time. Compared with the PZR pressure, the MSL pressure was decreased rapidly because coolant inventory in the secondary of SG was much smaller than primary coolant inventory. The SPACE prediction shows a good agreement with experiment data except for the asymmetric pressure behavior shown in experiment.

Similar to the PZR pressure behavior, the prediction of RCS coolant temperatures agreed well with experiment data as shown in Fig. 3. It means that the heat transfer coefficients for heat loss of overall system were determined appropriately. The RCS coolant temperature reached the safe shutdown condition around 100,000 seconds.

Fig. 4 shows the comparison of PZR water level between experiment and SPACE prediction. In the experiment, the PZR water level was continuously decreased due to the RCS cooling by heat loss and the cold CMT injection flow until 60,000 seconds. Till then, CMT injection was a forced circulation of single phase liquid flow through the PBL, CMT and injection lines because all RCPs were still running, therefore, it had little effect on the PZR water level. However, forced circulation through the PSIS lines was interrupted around 60,000 seconds because the PBL became empty as the RCS water level was decreased. Afterwards, the CMT injection by head difference between the PBLs and CMT injection lines began and as a result, the CMT water level was decreased as shown in Fig. 7, whereas the PZR water level was increased.

SPACE predicted such behavior of PZR water level very well but it was slowly recovered after 60,000 seconds compared with experiment data because the predicted CMT injection flow (Fig. 6) was smaller than experiment data.

The comparison of cold leg flow rate between experiment and SPACE prediction is shown in Fig. 5. As mentioned earlier, all RCPs were running for entire test period, so that the mass flow rate was almost the same as steady-state value. However, the measured flow rate was suddenly decreased right after the Rx trip but it is guessed that it resulted from improper density compensation when converting signal. Nevertheless, in SPACE simulation, the RCP speed was reduced by control logics to achieve the same cold leg flow rate as that of experiment. Fluctuations of flow rate shown in the experiment after 20,000 seconds are also caused by improper density compensation after the RCS condition reached saturated condition.

Fig. 6 shows the comparison of the PSIS flow rate including the CMTs and SITs. Forced circulation of single phase liquid flow by the RCPs in the early phase was interrupted after the PBL became empty and the CMT injection by head difference between the PBLs and CMT injection lines started around 60,000 seconds at loop #2 and around 85,000 seconds at loop #4 in experiment. However, in SPACE prediction, the interrupt of forced circulation occurred at the same time of 65,000 seconds in all loops and the CMT injection by head difference started around 70,000 seconds at loop #4 only. Consequently, the difference of CMT injection flow rate between SPACE and experiment caused the different increasing rate of the PZR water level (Fig. 4). SPACE also predicted the CMT injection flow at the loop #1 and #2 just before the SIT injection started.

Fig. 7 shows the comparison of the CMTs water level. Each CMT water level depends on the balance between the inflow from PBL and injection flow. Actual level decrease of CMTs in experiment occurred around 60,000 seconds after the PBL became empty as mentioned earlier. However, in SPACE simulation, decrease of the CMT water level is later than measured data as empty of PBL is delayed compared with experiment. Asymmetric level behavior observed in both experiment and SPACE resulted from the different PBL empty time of each loop.

3. Conclusions

The recently modified SPACE code for analysis of passive components such as CMT and SIT has been used to assess the TLOSHR scenario of the SMART-ITL and the effects of the heat loss and PSIS injection have been investigated. The predicted major parameters show reasonable agreements with the experiment and the sound capability of SPACE code.

ACKNOWLEDGEMENT

This research was supported by KAERI and King Abdullah City for Atomic and Renewable Energy (K.A.CARE), Kingdom of Saudi Arabia, within the Joint Research and Development Center.

REFERENCES

[1] J.H. Lee et al., PIRT development for Thermal-Hydraulic phenomena of SMART100-DECs, JRDC-TR-SP-20-17, 2020.
[2] H. Bae et al., Facility Description Report of FESTA, KAERI/TR-7294/2018.
[3] H. Bae et al., Data Analysis Report: Safety-Related Tests, S-750-NV-457-002 Rev.0, 2017.

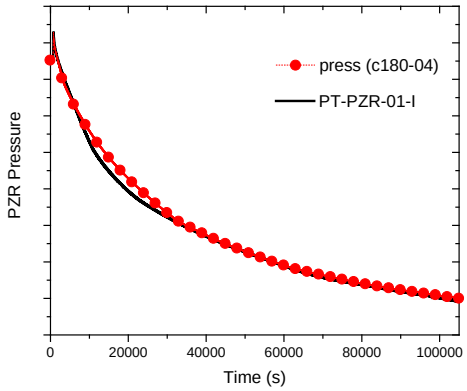

Fig. 1 Comparison of PZR Pressure

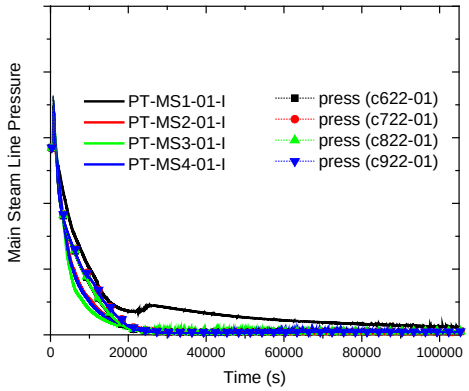

Fig. 2 Comparison of MSL Pressure

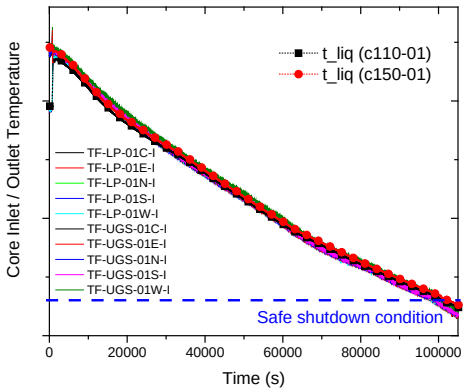

Fig. 3 Comparison of RCS Temperature

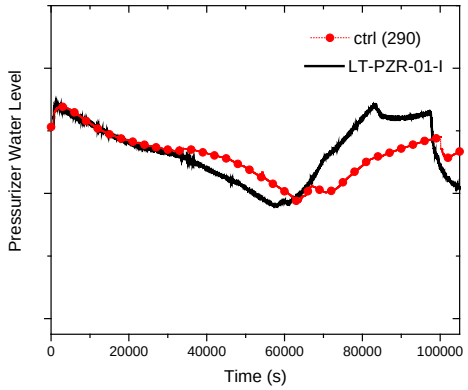

Fig. 4 Comparison of PZR Water Level

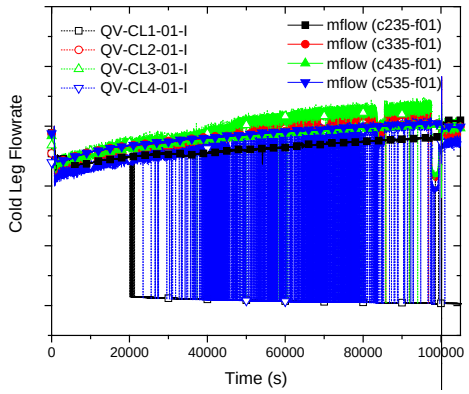

Fig. 5 Comparison of RCS Flowrate

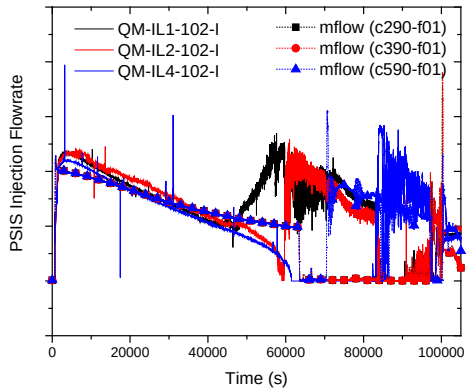

Fig. 6 Comparison of PSIS Injection

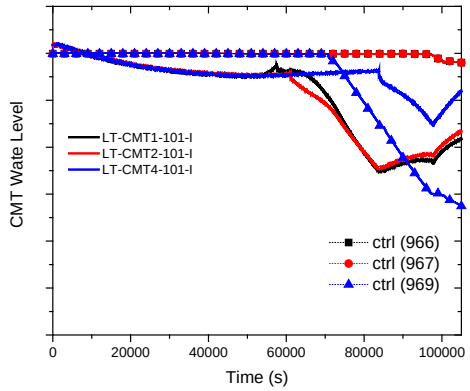

Fig. 7 Comparison of CMT Water Level